e-ISSN: 2689-4934

Available online at
http://uppp.uitm.edu.my/online-issues.html

ESTEEM Academic Journal Vol 20, March 2024, 24-35

ESTEEM
Academic Journal
(EAJ)

Biopolymer-based composite adsorbent beads for the removal of methylene blue dyes

Anis Nazira Alizan[1], Faraziehan Senusi[1*], Nurulhuda Amri[1], Mohammad Shahadat[2]

[1]*Chemical Engineering Studies, College of Engineering, Universiti Teknologi MARA, Cawangan Pulau Pinang, Permatang Pauh 13500, Malaysia*
[2]*School of Chemical Sciences, Univeristi Sains Malaysia, Penang 11800, Malaysia*

ARTICLE INFO

Article history:
Received 3 January 2024
Revised 8 March 2024
Accepted 22 March 2024
Online first
Published 29 March 2024

Keywords:
Biopolymer
Composite
Adsorption
Catecholamine
Beads
Dyes

DOI:
10.24191/esteem.v20iMarch.567.g473

ABSTRACT

Dyes containing waste streams are the most common pollutants found in wastewater, posing a severe threat to both the ecosystem and the environment. Adsorption emerges as one of the most effective and widely applied treatments for removing dyes due to its simple operation, high efficiency, and low cost. Sodium alginate, as a biopolymer, is one of the alternative adsorbents used in the adsorption process. However, the lack of active sites and low rigidity limits the adsorption capacity performance of this biopolymer. This study aims to introduce biopolymer-based composite adsorbent beads for removing methylene blue (MB) dye from an aqueous solution. Herein, TA/PANI/SA composite adsorbent beads consisting of tannic acid (TA) and polyaniline (PANI) were prepared by the cross-linking method of sodium alginate (SA) with the presence of divalent cations in calcium chloride. Characterization was performed using FTIR analysis to determine the changes in surface-modified composite beads. The results indicated that the removal efficiency of MB dye exhibited a significant enhancement of up to 72% when compared to untreated alginate beads, which only achieved approximately 30% removal. It was also found that the interactions occurred during the cross-linking process as well as during the adsorption process of MB dye onto the composite adsorbent beads. The adsorption mechanisms of MB dye by composite adsorbent beads include electrostatic interaction, π-π interactions, and hydrogen bonding. The improvement in the removal efficiency and the possibility of interactions during the cross-linking process suggested that the biopolymer-based composite beads have great potential to be used as adsorbents for removing dye in an aqueous solution.

[1*] Corresponding author. *E-mail address*: faraziehan@uitm.edu.my

https://doi.org/10.24191/esteem.v20iMarch.567.g473

1. INTRODUCTION

Water pollution has become a major environmental issue affecting organisms and ecosystems. Water pollution is caused by a variety of pollutants, including domestic wastewater [1], refinery and industrial wastewater [2], and agricultural activities [3]. Dye is one of the contaminants that contribute to water pollution, with industries related to dyes being textile, paper, dye synthesis, printing, leather, electroplating, plastic, paper, pharmaceutical, cosmetics, and food industries [4], [5]. The textile sector, for example, uses a lot of water in its processes, particularly for the wet processing of materials, and emits a lot of effluent into the environment [6]. The dye pollutant significantly impacts the environment, particularly in terms of polluting the ecosystem and endangering organisms [7]. When manufactured in high quantities, these dyes constitute a serious public health concern and the leading cause of harmful consequences in all living things. This is attributed to the discharge of highly coloured industrial dyes, which disrupt the ecological balance and harm aquatic species due to their low light transmittance and oxygen consumption. Moreover, they pose a risk to human health due to their bio-toxic and carcinogenic. Various technologies, including adsorption, are used for dye removal. Adsorption is regarded as one of the most feasible and successful water treatment methods. In terms of design flexibility and simplicity, starting cost, ease of operation, and sensitivity to harmful contaminants, adsorption has proven superior to alternative approaches [8].

Sodium alginate (SA), a natural biopolymer, has been successfully employed as an adsorbent because of the presence of a negatively charged carboxyl group. Alginate is used because it has a high affinity for ionic substances due to the presence of hydroxyl and carboxyl groups and its capability to form beads [9]. However, bare alginate polymer beads have several disadvantages, including a low surface area and a lack of active sites, which hinder internal active sites from contacting adsorbate molecules, especially affecting the swelling properties of bare alginate beads [10]. Composite beads are referred to as a type of material made up of cross-linked networks of hydrophilic polymer chains. Through cross-linking reactions, the number of active sites on the surface of the biopolymer can be increased, thereby enhancing the adsorption efficiency.

In this study, methylene blue (MB) was chosen as the synthetic dye pollutant due to its common cationic dyes, which are produced, especially by textile industries. Then, the modification to enhance the adsorption efficiency has been explored by the addition of a conductive polymer, polyaniline (PANI), in which the unique doping of PANI on biopolymer as adsorbent could enhance adsorbent-adsorbate interactions and adsorption performance [11]. In addition, the high degree of cross-linking of the copolymer PANI in the alginate must be considered. Therefore, tannic acid (TA), which is rich in catechol and pyrogallol groups, can serve as a versatile building block with a complex spectrum of chemical versatility, including self-polymerization, electrostatic interaction formation, and metal ion complexation [12]. Based on the above, it can be hypothesised that the oxidised TA under alkaline conditions could react with the amine and imine functional groups in PANI polymer chains to form a stable coordination complex in alginate.

2. MATERIALS AND METHODS

2.3 Materials

All chemicals used in this study were of analytical grade and used as received. Aniline ($C_6H_5NH_2$), ammonium persulfate ($(NH_4)_2S_2O_8$), sodium alginate and calcium chloride ($CaCl_2$) were purchased from QReC, Malaysia. Tris(hydroxymethyl)aminomethane (Tris-base) was supplied by Friendemann Schmidt Chemical. Tannic acid, methylene blue, hydrochloric acid (37%), and sodium hydroxide were purchased from Sigma-Aldrich.

https://doi.org/10.24191/esteem.v20iMarch.567.g473

2.3 Fabrication of composite adsorbent beads

A 2% w/v of PANI solution was prepared via the polymerization process by mixing the aniline and 0.1 M of ammonium persulfate as an oxidising agent into 1 M of hydrochloric acid solution. The mixing solution was prepared in the ice bath until the blue-green solution was formed and refrigerated for 24 hours. The resulting slurry was collected by vacuum filtration and rinsed with distilled water and ethanol for further use. Subsequently, a 2% w/v TA solution was prepared by dissolving tannic acid in pH 8.5 of 10 mM tris-HCl solution. The solution was mixed at constant agitation for three hours for the oxidation process, resulting in a change from a yellowish solution to a brownish colour. Similar steps were repeated to prepare 4% w/v of the TA solution. Then, the 2% w/v of SA solution was prepared by mixing sodium alginate into deionized water at room temperature until sodium alginate was well-dissolved. Then, the polyaniline was mixed into a TA solution. The mixed composite solution was added to the SA solution and stirred until a homogenous dispersion was formed. Next, the series of composite adsorbent beads were prepared using the cross-linking method. A similar size of beads was formed by dropping the mixed solution into 2% of calcium chloride with the help of a dropper. Finally, the beads were filtered and rinsed with distilled water several times and were kept in a distilled water bath for further use. The preparation of SA adsorbent without additives was carried out similarly, as illustrated in Fig. 1.

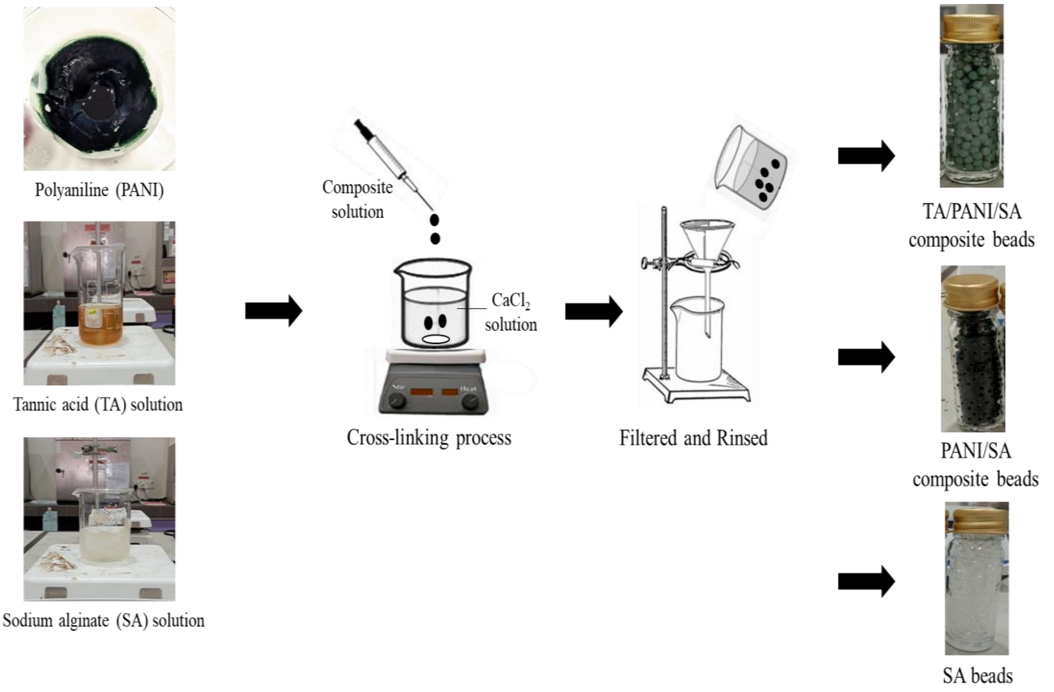

Fig. 1. Preparation of TA/PANI/Sa composite adsorbent beads

2.3 FTIR analysis

Fourier Transform Infrared Spectroscopy (FTIR) (Nicolet 6700, Thermo Fisher Scientific) was used to analyse the potential functional group present in the composite adsorbent beads. The measurement of the dry beads was conducted with solid slices within the wavelength range of 400 – 4000 cm^{-1}.

2.4 Adsorption performance analysis

For the adsorption study, 0.01 g/mL of a series of composite adsorbent beads was added into 50 mg/L of MB solutions. These solutions were then agitated at 150 rpm for two hours using an orbital shaker. The dye solution was analyzed at intervals of 30 minutes using a spectrophotometer (DR3900, Hach) at a wavelength of 664 nm. The adsorption capacity (q, mg/g) and removal efficiency (R, %) can be calculated as follows (Eq. (1) and Eq. (2)):

$$\mathrm{q} = \frac{(C_0 - C_e)V}{M} \tag{1}$$

$$\mathrm{R} = \frac{C_0 - C_e}{C_0} \times 100 \tag{2}$$

Where C_0 is the initial concentration of the dye solution (mg/L), C_e is the equilibrium concentration of the dye solution (mg/L), V is the volume of the dye solution (L), and M is the mass of adsorbent (mg). The analysis was further evaluated on the selected composite adsorbent beads with the highest removal efficiency during the adsorption study using the non-linear Langmuir and Freundlich isotherm models and Pseudo first and second-order kinetic models as shown in Table 1.

Table 1. Non-linear isotherm and kinetic adsorption model

Isotherm Model		**Parameters**
Langmuir	$q_e = \frac{q_{max} K_L C_e}{1 + K_L C_e}$ (3)	q_e = adsorption capacity at equilibrium $(\frac{mg}{g})$ q_{max} = monolayer coverage capacity $(\frac{mg}{g})$ K_L = Langmuir Isotherm constant $(\frac{L}{mg})$ K_F = Freundlich Isotherm constant $(\frac{L}{g})$ n = Adsorption intensity
Freundlich	$q_e = K_F$ (4)	
Kinetic Model		**Parameters**
Pseudo-first order	$q_t = q_e(1 - e^{(-K_1 t)})$ (5)	q_e = adsorption capacity at equilibrium $(\frac{mg}{g})$ q_t = adsoprtion capacity at time t $(\frac{mg}{g})$ K_1 = Rate constant of pseudo first $(\frac{g}{mg.min})$ K_2 = Rate constant of pseudo second $(\frac{g}{mg.min})$
Pseudo-second order	$q_t = \frac{q_e^2 K_2 t}{1 + q_e K_2 t}$ (6)	

The parameters and suitability of the models were evaluated using correlation of coefficient (R^2) and average relative error (ARE) analysis using Solver in Microsoft Excel (Eq. (3) and (Eq. (4).

$$R^2 = \frac{\sum(q_{e,cal} - q_{e,avg})^2}{\sum(q_{e,cal} - q_{e,avg})^2 + \sum(q_{e,cal} - q_{e,exp})^2} \tag{3}$$

$$ARE = \sum \left| \frac{q_{e,exp} - q_{e,cal}}{q_{e,exp}} \right| \tag{4}$$

https://doi.org/10.24191/esteem.v20iMarch.567.g473

3. RESULTS AND DISCUSSION

3.1 The possible mechanism of the cross-linked composite beads

Fig. 2 illustrates the possible mechanism of cross-linking between PANI chains and TA structures in the matrix of alginate. It is suggested that the catechol in the TA structure can form hydrogen bonds with the amine groups in PANI. Furthermore, the polyphenolic of TA, consisting of benzene rings, may form π-π interactions with the PANI chains, resulting in strengthening the bonding structures to the PANI surface. The complex compound of catechol in TA acts as an adhesive, facilitating reactions with other functional molecules to form a covalent network via chemical crosslinking [13]. It could also improve the interfacial bonding between additives and the polymer matrix [14]. Then, the cross-linking process of alginate with the PANI/TA additive occurred in the presence of divalent cations due to the strong interaction between the ions Ca^{2+} and COO^{-} groups. The alginates contain many free hydroxyl (–OH) and carboxyl (–COOH) groups, enabling them to form intramolecular hydrogen bonds in the gel matrix. Similar findings were reported by Li et al. on the intermolecular bonding that occurred between alginate and polydopamine [15].

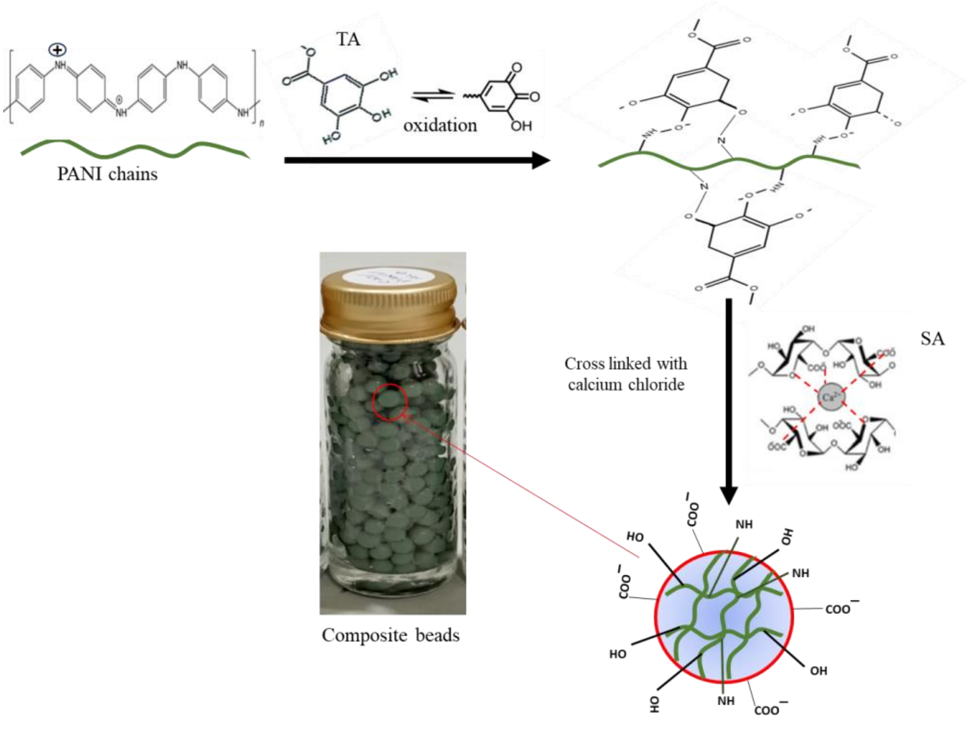

Fig. 2. Possible mechanism for the cross-linking process of TA/PANI/SA composite adsorbent beads

The surface functional groups of SA, PANI/SA, and TA/PANI/SA composite adsorbent beads were detected by FTIR spectroscopy, as shown in Fig. 3. The broad band within the range of 2800-3600 cm^{-1} from the spectrum of SA is attributed to the hydroxyl groups and -CH stretching. A strong and broad peak around this range arose due to the addition of the catechol (-OH) in TA and amine (-NH) stretching vibration of PANI. In addition, the O-H bend at 1415.5 cm^{-1} is significantly observed, which might be attributed to the overlapping peaks of hydroxyl groups in SA, suggesting the potential occurrence of hydrogen bonds during the process. Aziz et al. also reported that –OH peak stretching was observed after mixing alginate with clay, phosphate, and charcoal [16]. Moreover, the stretching vibration of carboxyl groups of SA beads at 1635.4 cm^{-1} slightly shifted to a low wavenumber, which might be attributed to the crosslinking process of TA and PANI in the alginate polymer matrix of SA. A similar finding by Peretz et al. reported that sodium alginate contains characteristic bands of hydroxyl at 3259 cm^{-1} and carboxyl at 1609 cm^{-1} for the spectra of sodium alginate and calcium alginate porous beads [17]. The addition of PANI as an additive in the alginate beads clearly shows the C-N stretching vibration of the benzenoid ring at the peak of 1336.4 cm^{-1} [18]. The spectrum at a range of 900-1100 cm^{-1} occurred for the C=O group of alginate, in which the intensity increased in the spectra of composite beads [19]. Based on a study conducted by Janaki et al., it was stated that the presence of functional groups, which are amine, hydroxyl, and carboxyl groups improved the adsorption efficiency of St-PANI nanocomposite [20].

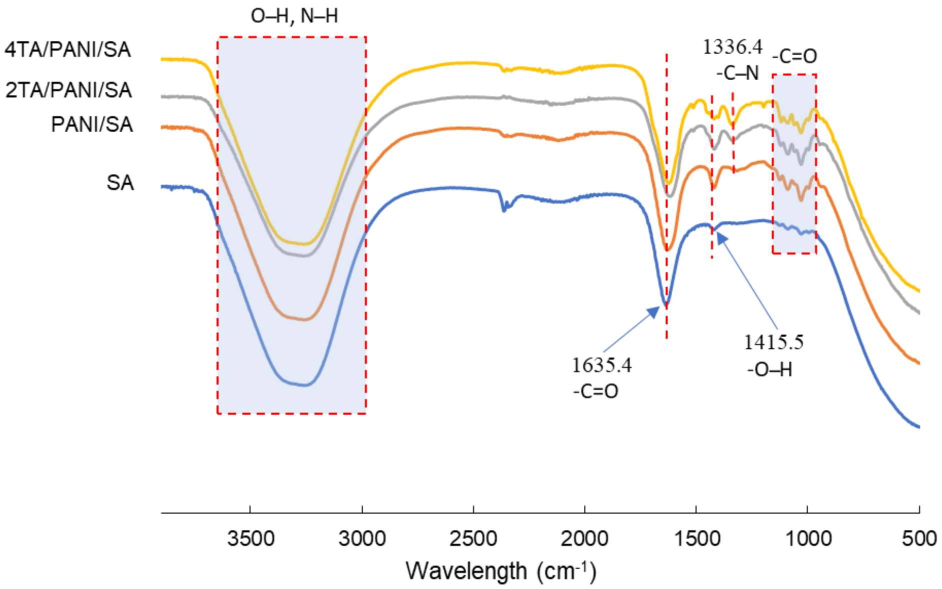

Fig. 3. FTIR spectroscopy of SA, PANI/SA, 2% and 4% TA/PANI/SA composite adsorbent beads

3.2 Adsorption analysis of composite adsorbent beads

Fig. 4 shows the adsorption capacity and removal efficiency of MB dye onto the series of adsorbent beads. The 4%TA/PANI/SA shows the highest removal efficiency, followed by 2%TA/PANI/SA and PANI/SA adsorbent beads. It can be seen that the TA and PANI contents have the greatest influence on the adsorption performance compared to the pristine alginate beads. Due to the abundance of phenolic hydroxyl groups on TA, which are capable of hydrolysing to anions (-O-) under basic conditions, the adsorption capacity of the composite adsorbent beads increases and the interaction with MB dye strengthens. A similar finding was reported on the properties of activated hydrochar encapsulated in the alginate particles [21]. In addition, the removal efficiency increased with increasing the ratio of catechol in composite adsorbent beads. This may be due to the interaction of active groups between catechol and PANI during the cross-linking process. These results align with another study in which the ratio of catechol to amine groups influences the interaction during the cross-linking process [22-23]. Hu et al. stated that the increasing TA content on TA-PVA/SA hydrogel beads led to a gradual rise in the adsorption capacity of MB dye. This is because the composite adsorbent beads adsorbed more MB dye when there are more −OH sites in the adsorbents [24].

https://doi.org/10.24191/esteem.v20iMarch.567.g473

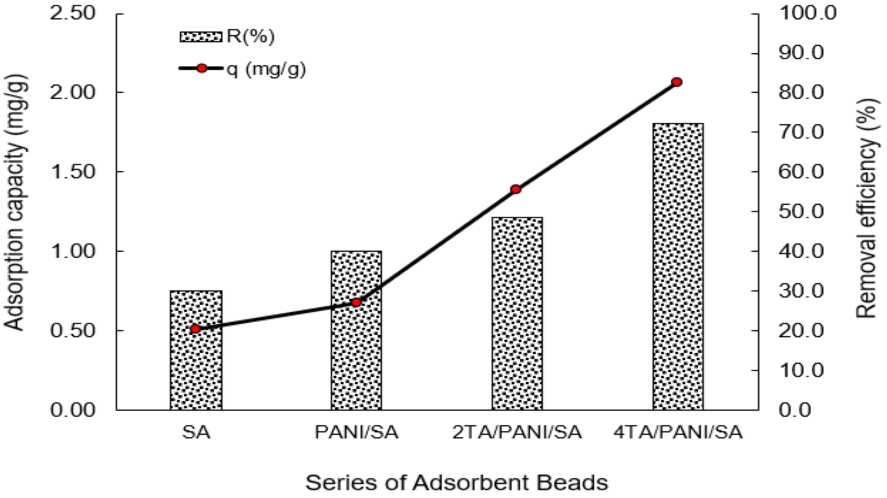

Fig. 4. Adsorption capacity and removal efficiency of composite adsorbent beads

The changes in the functional group indicate the adsorption process that occurred on composite adsorbent beads, as presented in Fig. 5. After the adsorption of MB dye, the significant changes on the peak at 1336.4 cm^{-1} attributed to C-N groups were observed as shifted to a higher wavelength at 1421.3 cm^{-1}, which might be due to the accumulation of MB dyes on the surface of 4%TA/PANI/ALG composite beads [25]. The electrostatic attraction could occur between N$^+$ of MB dyes and O$^-$ and COO$^-$ of composite adsorbent beads, indicating the disappearance of OH bend vibration. The decreasing peak intensities at the range of 900-1100 cm^{-1} were also observed due to the electrostatic interactions during the adsorption process.

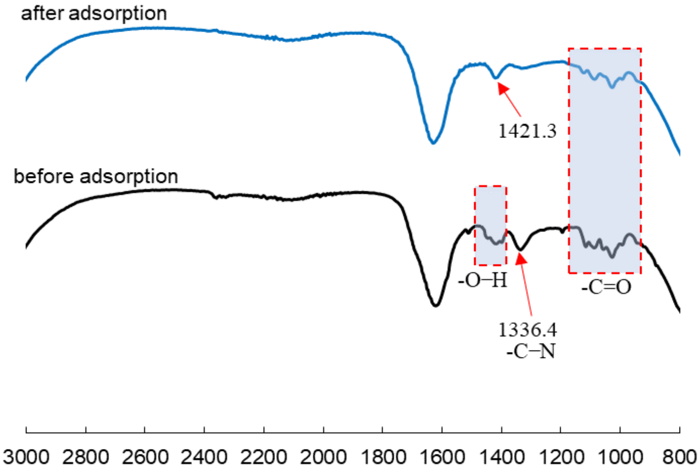

Fig. 5. Adsorption capacity and removal efficiency of composite adsorbent beads

https://doi.org/10.24191/esteem.v20iMarch.567.g473

In addition, π-π interaction also occurred between the ring structures of TA and polyaniline during the adsorption of MB dye. Nasar et al. stated that typically, multiple iterations are accomplished during dye adsorption on polyaniline-based materials through the π-π interaction, electrostatic attraction, and hydrogen bonding [26]. A possible mechanism during the MB dye adsorption process on the TA/PANI/SA composite adsorbent beads is suggested in Fig. 6.

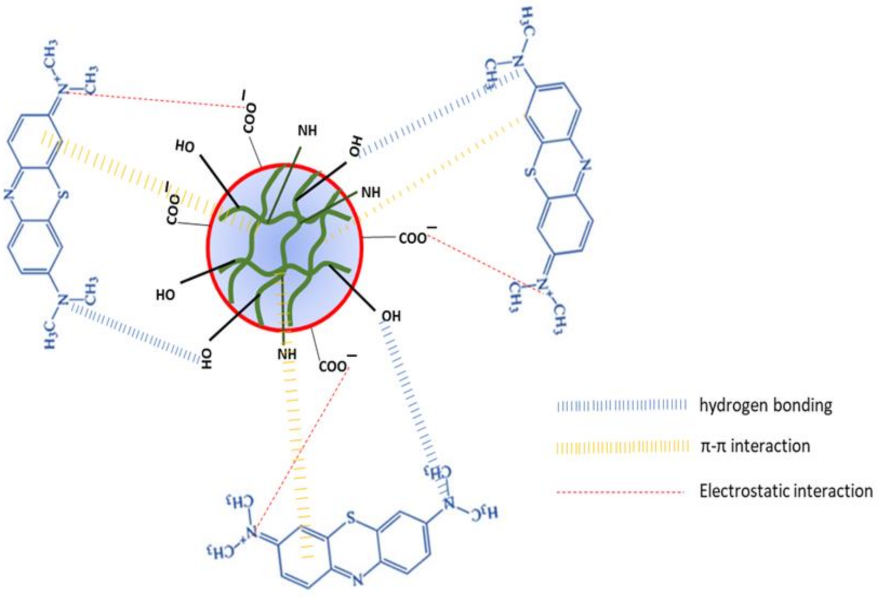

Fig. 6. The plausible interaction between TA/PANI/SA composite adsorbent beads with structures of MB dye

3.3 Evaluation of adsorption isotherm and kinetic model

The adsorption isotherm was used to describe the interactive behaviour between the adsorbate and the adsorbent. The experimental data for different initial concentrations was fitted to nonlinear Langmuir and Freundlich isotherms models. The Langmuir model describes the adsorption of a single layer on a homogeneous surface, while the multilayer adsorption on a heterogeneous surface can be suggested by the Freundlich adsorption isotherm. Using nonlinear regression is the best way to calculate the isotherm parameters, as these should be used in their original forms according to Eq. (3) and Eq. (4), respectively. The graphs of both isotherms are shown in Fig. 7, and the calculated model parameters are presented in Table 2.

Table 2. Nonlinear parameter model for adsorption isotherm model for removal of MB dye by 4%TA/PANI/SA composite adsorbent beads

Langmuir Model		**Freundlich Model**	
q_{max}	1.176	1/n	0.221
K_L	0.174	K_F	0.440
R^2	0.788	R^2	0.682
ARE	0.249	ARE	0.381

https://doi.org/10.24191/esteem.v20iMarch.567.g473

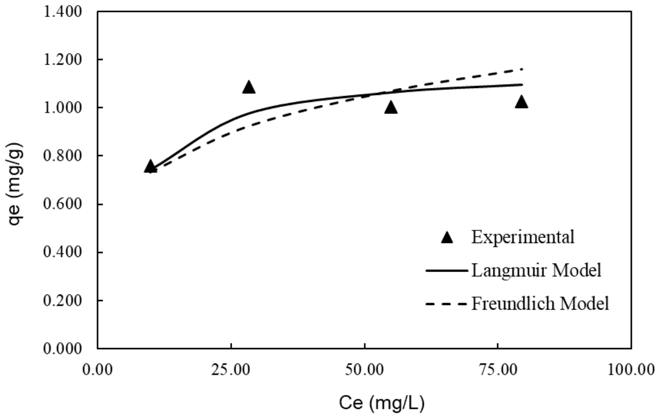

Fig. 7. Nonlinear adsorption isotherm model for removal of MB dye by 4%TA-PANI/SA composite adsorbent beads.

According to the average relative error (ARE) and correlation of determination (R^2) values, the Langmuir model fitted the experimental data better than the Freundlich isotherms model. It indicated that MB cationic dye adsorption demonstrated monolayer coverage on the active sites of the adsorbent beads. In addition, the Langmuir isotherm can be used to predict the separation factor (R_L), which shows whether the adsorption process is favourable ($0 < R_L < 1$) or unfavourable ($R_L > 1$) [27]. In this study, the calculated value of R_L was between 0.05 and 0.19, demonstrating the favourable adsorption process.

The adsorption kinetics were applied to define the effectiveness of the adsorption process based on the rate of removal of solute, which controls the stay period of the MB dye at the interface of the solid solution. The parameter of adsorption kinetics was calculated by fitting the experimental data at different times to a nonlinear form of pseudo-first order (Eq. 5) and pseudo-second order (Eq. 6), as plotted in Fig. 8. It can be seen that the initial rate of MB adsorption rapidly increased and reached equilibrium after 90 min due to the saturation of the adsorbent. Higher initial concentrations of MB dye show an increment in adsorption capacity, which could be due to excessive driving force between the liquid and solid phase and reflect an efficient utilisation of adsorbent sites [28].

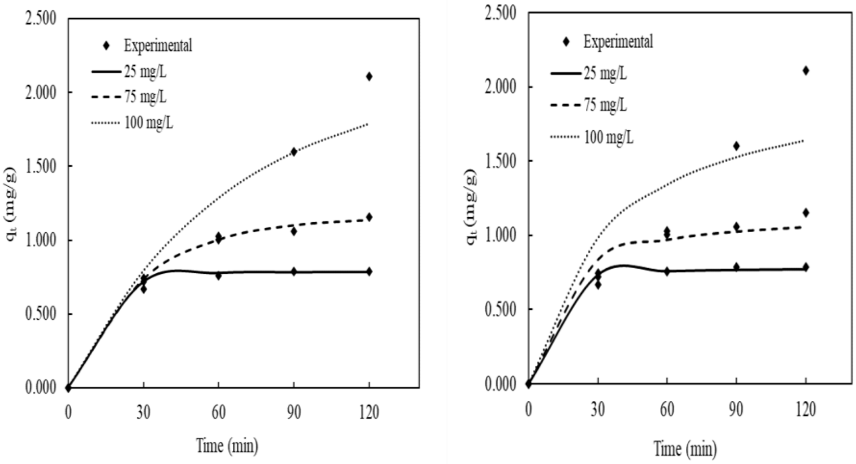

Fig. 8. Nonlinear pseudo first (a) and second order (b) kinetic model for removal of MB dye by 4%TA/PANI/SA composite adsorbent beads.

https://doi.org/10.24191/esteem.v20iMarch.567.g473

The calculated model parameters are presented in Table 3. According to the ARE and R^2 values, the experimental data fit well with the pseudo-first order models. It was suggested that the physical interaction of adsorbent surface sites via electrostatic attractions between the negative charge on the composite adsorbent and $^+N(CH_3)_2$ of the cationic dye, as well as hydrogen bonding, played a significant role in the MB adsorption removal process [29].

Table 3. Nonlinear parameters for adsorption kinetic model for removal of MB dye by 4%TA/PANI/SA composite adsorbent beads

Kinetic Model	**Pseudo First Order**			**Pseudo Second order**		
Initial Concentration	25 mg/L	75 mg/L	100 mg/L	25 mg/L	75 mg/L	100 mg/L
R^2	0.999	0.997	0.918	0.999	0.974	0.806
ARE	0.033	0.074	0.585	0.055	0.275	1.038
k	4.950	2.014	0.937	36.023	4.497	0.824

4. CONCLUSION

In this work, TA/PANI/SA composite adsorbent beads were synthesised via the cross-linking process of polyaniline and tannic acid as additives in the matrix of alginate for the adsorption of methylene blue dye. This study found an increased removal efficiency of MB dye when using the TA/PANI/SA composite adsorbent beads as compared with the SA beads. For the effect of the TA ratio in the composite adsorbent beads, the highest ratio has the greatest influence on the MB dye removal due to the increasing groups of active sites in the adsorbents. A further assessment conducted via FTIR analysis suggests potential enhancement of the functional groups of the TA/PANI/SA composite adsorbent beads, supporting the multiple interactions that could occur during the interaction with the structure of MB dye. The results obtained from the Langmuir isotherm and pseudo-first order kinetic adsorption models suggested that the physical interactions occurred during the adsorption process. Therefore, for further work, additional characterizations such as FESEM and BET analysis and desorption studies should be considered to describe the morphology and reusability of the composite adsorbent beads.

5. ACKNOWLEDGEMENT

This study was funded by Ministry of Higher Education through Fundamental Research Grant Scheme (FRGS/1/2023/TK09/UITM/02/1). The authors acknowledge Universiti Teknologi MARA, Cawangan Pulau Pinang, Malaysia for the facility support throughout this research work.

6. CONFLICT OF INTEREST STATEMENT

The authors agree that this research was conducted in the absence of any self-benefits, commercial or financial conflicts and declare the absence of conflicting interests with the funders.

7. AUTHORS’ CONTRIBUTIONS

Anis Nazira Alizan: Conceptualisation, lab work, investigation and formal analysis, writing-original draft; **Faraziehan Senusi**: Conceptualisation, formal analysis, supervision, and writing and editing; **Nurulhuda Amri**: Conceptualisation, formal analysis, and validation; **Mohammad Shahadat**: Conceptualisation, supervision and validation.

https://doi.org/10.24191/esteem.v20iMarch.567.g473

8. REFERENCES

[1] J. Zhao *et al.*, “PVDF membrane was modified by hydroxymethylated lignin to improve its hydrophilicity in treating oily wastewater,” *Mater. Today Commun.*, vol. 35, no. April, 2023. Available: doi: 10.1016/j.mtcomm.2023.106055.

[2] K. K. H. Dizayee and S. J. Judd, “A Brief Review of the Status of Low-Pressure Membrane Technology Implementation for Petroleum Industry Effluent Treatment,” *Membranes (Basel).*, vol. 12, no. 4, 2022. Available: doi: 10.3390/membranes12040391.

[3] L. Schweitzer and J. Noblet, “Water Contamination and Pollution,” in *Green Chemistry*, Elsevier, pp. 261–290, 2018. Available: doi: 10.1016/B978-0-12-809270-5.00011-X.

[4] S. K. Yadav, S. R. Dhakate, and B. Pratap Singh, “Carbon nanotube incorporated eucalyptus derived activated carbon-based novel adsorbent for efficient removal of methylene blue and eosin yellow dyes,” *Bioresour. Technol.*, vol. 344, p. 126231, Jan. 2022. Available: doi: 10.1016/j.biortech.2021.126231.

[5] I. Dalponte Dallabona, Á. L. Mathias, and R. M. M. Jorge, “A new green floating photocatalyst with Brazilian bentonite into TiO2/alginate beads for dye removal,” *Colloids Surfaces A Physicochem. Eng. Asp.*, vol. 627, p. 127159, Oct. 2021, doi: 10.1016/j.colsurfa.2021.127159.

[6] K. O. Iwuozor, J. O. Ighalo, E. C. Emenike, L. A. Ogunfowora, and C. A. Igwegbe, “Adsorption of methyl orange: A review on adsorbent performance,” *Curr. Res. Green Sustain. Chem.*, vol. 4, p. 100179, 2021. Available: doi: 10.1016/j.crgsc.2021.100179.

[7] S. Xu, Y. Jin, R. Li, M. Shan, and Y. Zhang, “Amidoxime modified polymers of intrinsic microporosity/alginate composite hydrogel beads for efficient adsorption of cationic dyes from aqueous solution,” *J. Colloid Interface Sci.*, vol. 607, pp. 890–899, Feb. 2022. Available: doi: 10.1016/j.jcis.2021.08.157.

[8] N. B. Singh, G. Nagpal, S. Agrawal, and Rachna, “Water purification by using Adsorbents: A Review,” *Environ. Technol. Innov.*, vol. 11, pp. 187–240, 2018, doi: 10.1016/j.eti.2018.05.006.

[9] M. Hassan *et al.*, “Magnetically separable mesoporous alginate polymer beads assist adequate removal of aqueous methylene blue over broad solution pH,” *J. Clean. Prod.*, vol. 319, p. 128694, Oct. 2021. Available: doi: 10.1016/j.jclepro.2021.128694.

[10] B. Wang *et al.*, “Alginate-based composites for environmental applications: a critical review,” *Crit. Rev. Environ. Sci. Technol.*, vol. 49, no. 4, pp. 318–356, Feb. 2019. Available: doi: 10.1080/10643389.2018.1547621.

[11] M. Shahadat *et al.*, “A critical review on the prospect of polyaniline-grafted biodegradable nanocomposite,” *Adv. Colloid Interface Sci.*, vol. 249, pp. 2–16, Nov. 2017. Available: doi: 10.1016/j.cis.2017.08.006.

[12] H. Xie *et al.*, “Efficient oil-water emulsion treatment via novel composite membranes fabricated by CaCO3-based biomineralization and TA-Ti(IV) coating strategy,” *Sci. Total Environ.*, vol. 857, no. September 2022. Available: doi: 10.1016/j.scitotenv.2022.159183.

[13] C. Chen, H. Yang, X. Yang, and Q. Ma, “Tannic acid: A crosslinker leading to versatile functional polymeric networks: A review,” *RSC Adv.*, vol. 12, no. 13, pp. 7689–7711, 2022. Available: doi: 10.1039/d1ra07657d.

[14] Y. Wei *et al.*, “A soy protein-based adhesive with improved mechanical and electromagnetic shielding properties by employment of core@double-shell BT@PDA@PANI fillers,” *Chem. Eng. J.*, vol. 458, p. 141512, Feb. 2023. Available: doi: 10.1016/j.cej.2023.141512.

[15] X. Li, H. Lu, Y. Zhang, F. He, L. Jing, and X. He, “Fabrication of magnetic alginate beads with uniform dispersion of CoFe2O4 by the polydopamine surface functionalization for organic pollutants removal,” *Appl. Surf. Sci.*, vol. 389, pp. 567–577, Dec. 2016. Available: doi: 10.1016/j.apsusc.2016.07.162.

[16] F. Aziz *et al.*, “Composites with alginate beads: A novel design of nano-adsorbents impregnation for large-scale continuous flow wastewater treatment pilots,” *Saudi J. Biol. Sci.*, vol. 27, no. 10,

https://doi.org/10.24191/esteem.v20iMarch.567.g473

pp. 2499–2508, Oct. 2020. Available: doi: 10.1016/j.sjbs.2019.11.019.
[17] S. Peretz, D. F. Anghel, E. Vasilescu, M. Florea-Spiroiu, C. Stoian, and G. Zgherea, “Synthesis, characterization and adsorption properties of alginate porous beads,” *Polym. Bull.*, vol. 72, no. 12, pp. 3169–3182, Dec. 2015. Available: doi: 10.1007/s00289-015-1459-4.
[18] J. Ding, W. Zhang, X. Dai, J. Yao, and G. Gao, “Synchronous removal and separation of multiple contaminants by poly (vinylidene fluoride)/polyaniline ultrafiltration membrane,” *J. Environ. Chem. Eng.*, vol. 10, no. 6, p. 108926, Dec. 2022. Available: doi: 10.1016/j.jece.2022.108926.
[19] M. Z. I. Mollah, M. R. I. Faruque, D. A. Bradley, M. U. Khandaker, and S. Al Assaf, “FTIR and rheology study of alginate samples: Effect of radiation,” *Radiat. Phys. Chem.*, vol. 202, no. September 2022. Available: doi: 10.1016/j.radphyschem.2022.110500.
[20] V. Janaki *et al.*, “Starch/polyaniline nanocomposite for enhanced removal of reactive dyes from synthetic effluent,” *Carbohydr. Polym.*, vol. 90, no. 4, pp. 1437–1444, 2012. Available: doi: 10.1016/j.carbpol.2012.07.012.
[21] T. P. de Araújo *et al.*, “Acetaminophen removal by calcium alginate/activated hydrochar composite beads: Batch and fixed-bed studies,” *Int. J. Biol. Macromol.*, vol. 203, no. January, pp. 553–562, Apr. 2022. Available: doi: 10.1016/j.ijbiomac.2022.01.177.
[22] D. Li *et al.*, “Application of a Catechol-Polyamine Co-Deposition method for synthesis of Heteroatom-Doped carbon nanomaterials,” *Chem. Eng. J.*, vol. 429, no. July 2021, p. 132363, Feb. 2022. Available: doi: 10.1016/j.cej.2021.132363.
[23] F. Senusi, N. Nasuha, A. Husain, and S. Ismail, “Synthesis of catechol-amine coating solution for membrane surface modification,” *Environ. Sci. Pollut. Res.*, vol. 30, no. 60, pp. 124585–124595, May 2022. Available: doi: 10.1007/s11356-022-20167-4.
[24] T. Hu, Q. Liu, T. Gao, K. Dong, G. Wei, and J. Yao, “Facile Preparation of Tannic Acid–Poly(vinyl alcohol)/Sodium Alginate Hydrogel Beads for Methylene Blue Removal from Simulated Solution,” *ACS Omega*, vol. 3, no. 7, pp. 7523–7531, Jul. 2018. Available: doi: 10.1021/acsomega.8b00577.
[25] S. F. F. Azha, A. L. L. Ahmad, and S. Ismail, “Thin coated adsorbent layer: characteristics and performance study,” *Desalin. Water Treat.*, vol. 55, no. 4, pp. 956–969, Jul. 2015. Available: doi: 10.1080/19443994.2014.922502.
[26] A. Nasar and F. Mashkoor, “Application of polyaniline-based adsorbents for dye removal from water and wastewater—a review,” *Environ. Sci. Pollut. Res.*, vol. 26, no. 6, pp. 5333–5356, Feb. 2019. Available: doi: 10.1007/s11356-018-3990-y.
[27] A. Benhouria, H. Zaghouane-Boudiaf, R. Bourzami, F. Djerboua, B. H. Hameed, and M. Boutahala, “Cross-linked chitosan-epichlorohydrin/bentonite composite for reactive orange 16 dye removal: Experimental study and molecular dynamic simulation,” *Int. J. Biol. Macromol.*, vol. 242, p. 124786, Jul. 2023. Available: doi: 10.1016/j.ijbiomac.2023.124786.
[28] M. H. Dehghani, S. Afsari Sardari, M. Afsharnia, M. Qasemi, and M. Shams, “Removal of toxic lead from aqueous solution using a low-cost adsorbent,” *Sci. Rep.*, vol. 13, no. 1, p. 3278, Feb. 2023. Available: doi: 10.1038/s41598-023-29674-x.
[29] O. B. Nchoe, S. O. Sanni, E. L. Viljoen, A. Pholosi, and V. E. Pakade, “Surfactant-modified Macadamia nutshell for enhancement of methylene blue dye adsorption from aqueous media,” *Case Stud. Chem. Environ. Eng.*, vol. 8, p. 100357, Dec. 2023. Available: doi: 10.1016/j.cscee.2023.100357.

https://doi.org/10.24191/esteem.v20iMarch.567.g473